Science Translational Medicine
AAAS

Supplementary Materials for

Antibody-mediated prevention of vaginal HIV transmission is dictated by IgG subclass in humanized mice

Jacqueline M. Brady *et al.*

Corresponding author: Alejandro B. Balazs, abalazs@mgh.harvard.edu

Sci. Transl. Med. **14**, eabn9662 (2022)
DOI: 10.1126/scitranslmed.abn9662

The PDF file includes:

Other Supplementary Material for this manuscript includes the following:

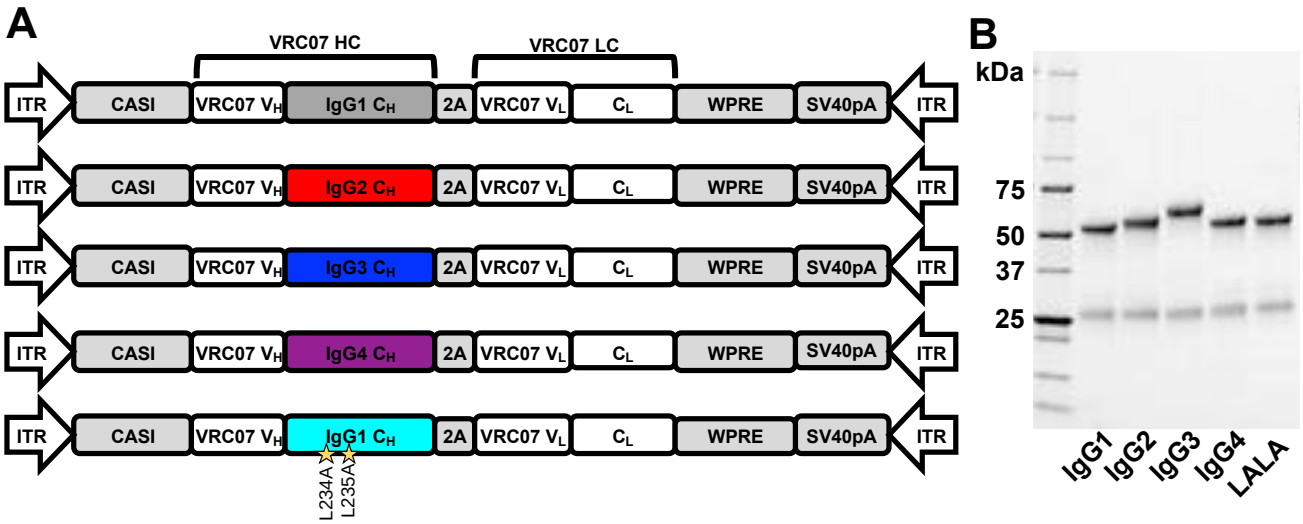

Figure S1. Expression and purification of VRC07 IgG subclasses.
(**A**) Schematic representations of the adeno-associated virus (AAV) vectors used for in vivo expression of VRC07 IgG subclasses; the vectors include inverted terminal repeats (ITR), CASI promoter, various VRC07 IgG heavy chains (HC) linked to the VRC07 kappa light chain separated by a self-processing 2A sequence, Woodchuck Hepatitis Virus Posttranscriptional Regulatory Element (WPRE) for improved expression, and an SV40 late-polyadenylation signal.
(**B**) SDS-PAGE of purified VRC07 IgG subclasses, 1 µg of each variant under reducing conditions. VRC07 light chains are observed at 26 kDa and VRC07 heavy chains vary by constant region subclass from 50 to 60 kDa.

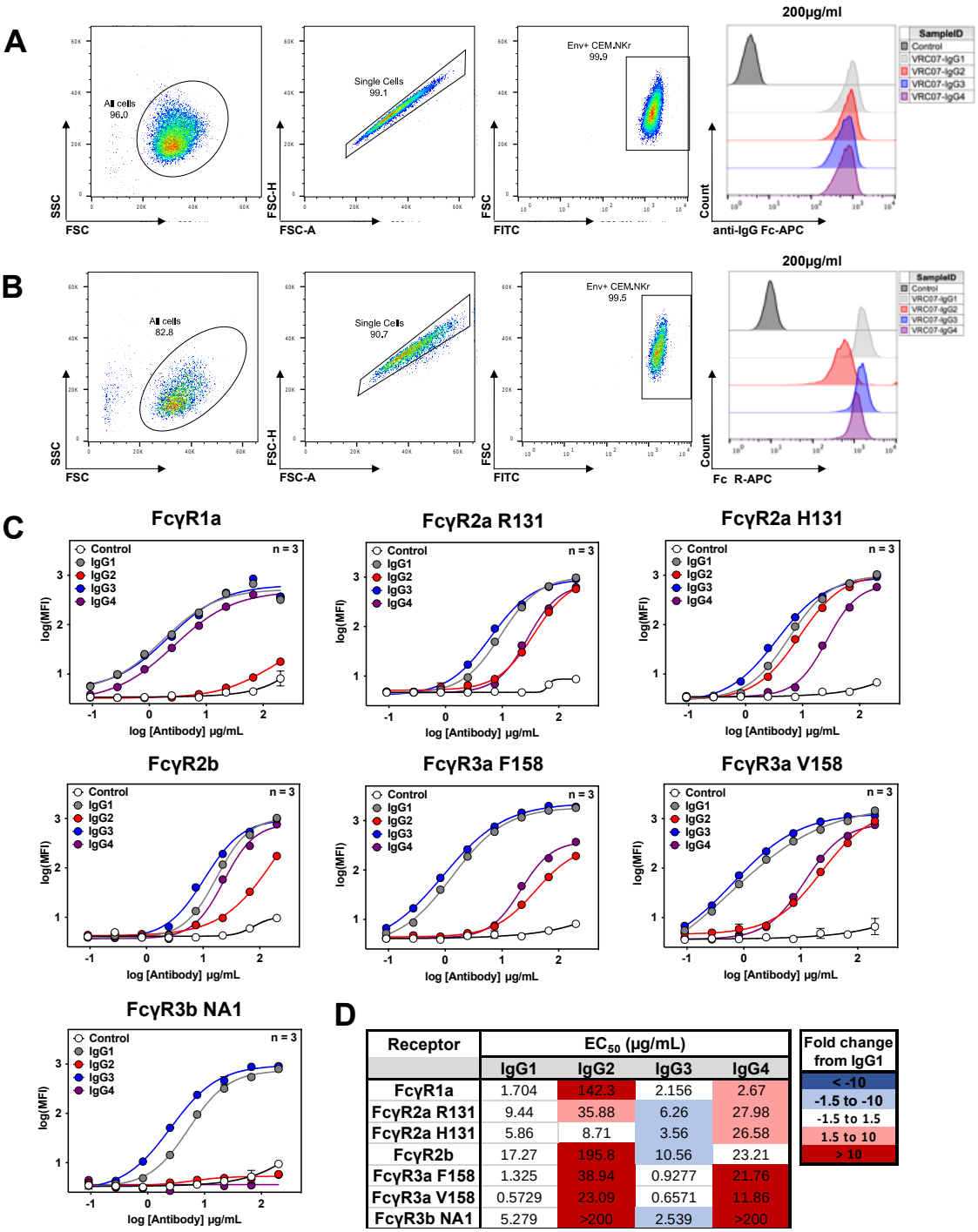

Receptor	EC_{50} (µg/mL)			
	IgG1	IgG2	IgG3	IgG4
FcγR1a	1.704	142.3	2.156	2.67
FcγR2a R131	9.44	35.88	6.26	27.98
FcγR2a H131	5.86	8.71	3.56	26.58
FcγR2b	17.27	195.8	10.56	23.21
FcγR3a F158	1.325	38.94	0.9277	21.76
FcγR3a V158	0.5729	23.09	0.6571	11.86
FcγR3b NA1	5.279	>200	2.539	>200

Fold change from IgG1
< -10
-1.5 to -10
-1.5 to 1.5
1.5 to 10
> 10

Figure S2. VRC07 IgG subclasses differentially bind to Fc gamma receptor (FcγR) proteins.
(**A**) Gating strategy for binding assay to HIV_{JR-CSF} Env-expressing target cells comparing allophycocyanin (APC)-labeled VRC07 IgG subclasses. A representative example is shown using a concentration of 200 µg/ml of each subclass. Forward Scatter (FSC), Side Scatter (SSC), Fluorescein isothiocyanate (FITC), Allophycocyanin (APC)
(**B**) Gating strategy for FcγR binding assay comparing the interactions of various FcγR proteins to VRC07 IgG subclasses bound to HIV_{JR-CSF} envelope (Env)-expressing target cells. A representative example is shown using a concentration of 200 µg/ml of each subclass.
(**C**) FcγR binding profiles for VRC07 IgG subclasses bound to HIV_{JR-CSF} Env-expressing CEM.NKr cells as measured by flow cytometry (*n* = 3 per group). The control is a non-HIV-specific IgG1 antibody. Error bars represent standard error of the mean (SEM).
(**D**) EC_{50}, or half-maximal binding concentrations (µg/mL) calculated for each VRC07 IgG subclass and FcγR combination. The color of the box indicates the fold change in half-maximal binding (EC_{50}) compared to VRC07 IgG1.

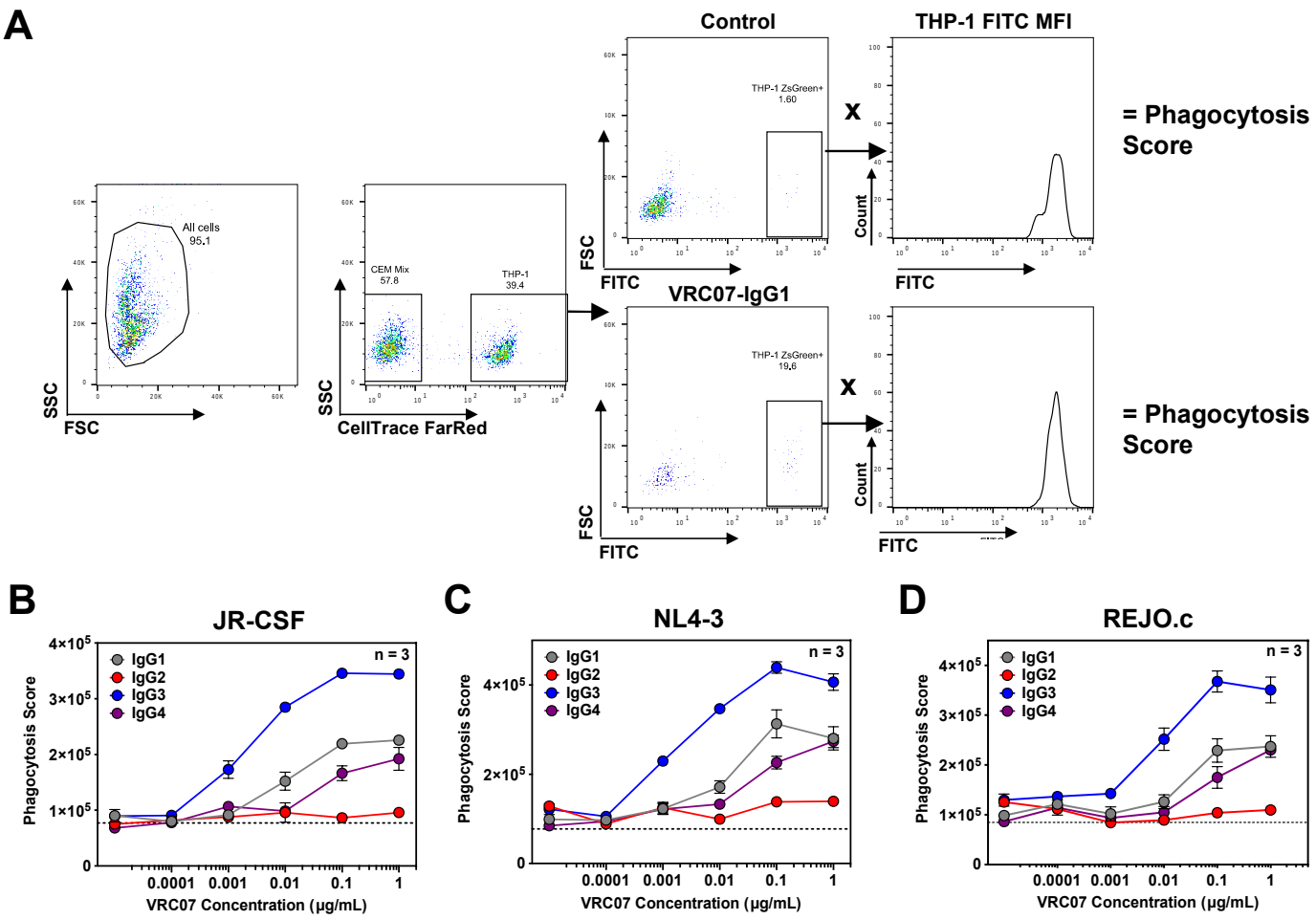

Figure S3. IgG subclass impacts the ability of VRC07 to mediate antibody-dependent cellular phagocytosis (ADCP) by THP-1 cells.

(**A**) Gating strategy of THP-1-based ADCP assay comparing the activity of either a control antibody or VRC07 IgG1 against $HIV_{JR\text{-}CSF}$ Env-expressing target cells. A representative example is shown using a concentration of 1 µg/ml of either antibody. Phagocytosis score is determined by multiplying the percentage of $ZsGreen^{+}$ THP-1 cells and their mean fluorescence intensity (MFI).

(**B** to **D**) Phagocytosis of $HIV_{JR\text{-}CSF}$ (B), $HIV_{NL4\text{-}3}$ (C), or $HIV_{REJO.c}$ (D) gp120-coated fluorescent beads by THP-1 cells in the presence of different VRC07 IgG subclasses as measured by flow cytometry. The dotted lines indicates the average phagocytic score in the absence of a VRC07 subclass antibody (*n* = 3 per group).

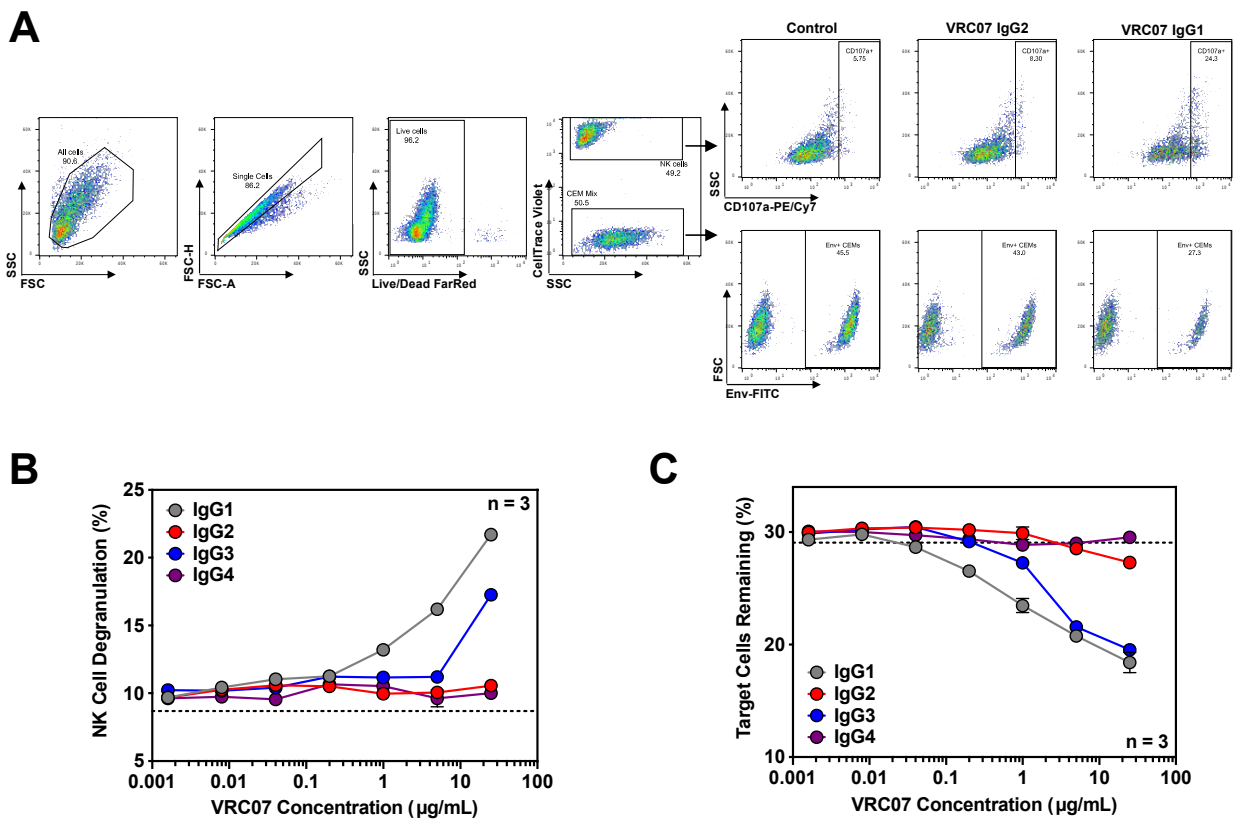

Figure S4. VRC07 IgG subclasses demonstrate differential ability to mediate antibody-dependent cellular cytotoxicity (ADCC).

(**A**) Gating strategy of primary natural killer (NK) cell-based ADCC assay comparing the capacity of VRC07 IgG subclasses to mediate both degranulation (CD107a) and elimination of $HIV_{JR\text{-}CSF}$ Env-expressing target cells. A representative example is shown using a concentration of 25 µg/ml of a malaria-specific negative control IgG1, VRC07 IgG2 or VRC07 IgG1. FSC-H: Forward Scatter Height, SSC-H: Side Scatter Height, FSC-A: Forward Scatter Area, PE: Phycoerythrin, Cy7: Cyanine 7, FITC: Fluorescein isothiocyanate

(**B** and **C**) Ability of VRC07 IgG subclasses to mediate NK cell degranulation (B) as well as specific killing of $HIV_{JR\text{-}CSF}$ Env-expressing target cells (C) as measured by flow cytometry (n = 3 per group). Results are from a genetically-distinct NK cell donor than those in Fig. 1. The dotted line indicates the average value in the absence of a VRC07 subclass antibody. Error bars represent SEM.

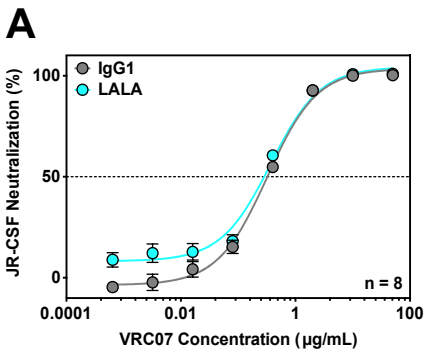

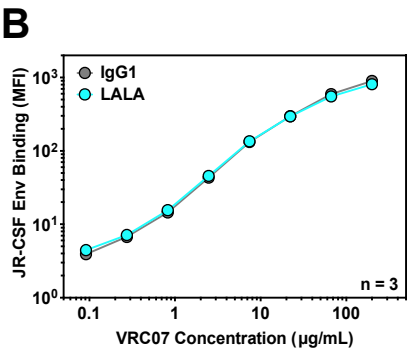

C

Receptor	EC_{50} (µg/mL)	
	IgG1	LALA
FcγR1a	1.704	10.86
FcγR2a R131	9.44	>200
FcγR2a H131	5.86	124.9
FcγR2b	17.27	>200
FcγR3a F158	1.325	11.17
FcγR3a V158	0.5729	4.44
FcγR3b NA1	5.279	43.89

Fold change from IgG1
< -10
-1.5 to -10
-1.5 to 1.5
1.5 to 10
> 10

Figure S5. **Impact of L234A, L235A (LALA) mutations on neutralization, Env binding, and FcγR binding of VRC07 IgG1.**
(**A**) In vitro neutralization activity of purified VRC07 IgG1 or LALA against $HIV_{JR\text{-}CSF}$ as measured by TZM-bl neutralization assays (*n* = 8 per group). Error bars represent SEM.
(**B**) Binding of VRC07 IgG1 or LALA to $HIV_{JR\text{-}CSF}$ Env-expressing target cells as measured by flow cytometry with a pan-IgG-Fc detection reagent (*n* = 3 per group). Error bars represent SEM.
(**C**) Half-maximal binding concentration (EC_{50}) of cell surface-bound VRC07 IgG1 or LALA to purified fluorescent-labeled FcγR proteins as measured by flow cytometry. The color of the box indicates the fold change in half-maximal binding compared to VRC07 IgG1.

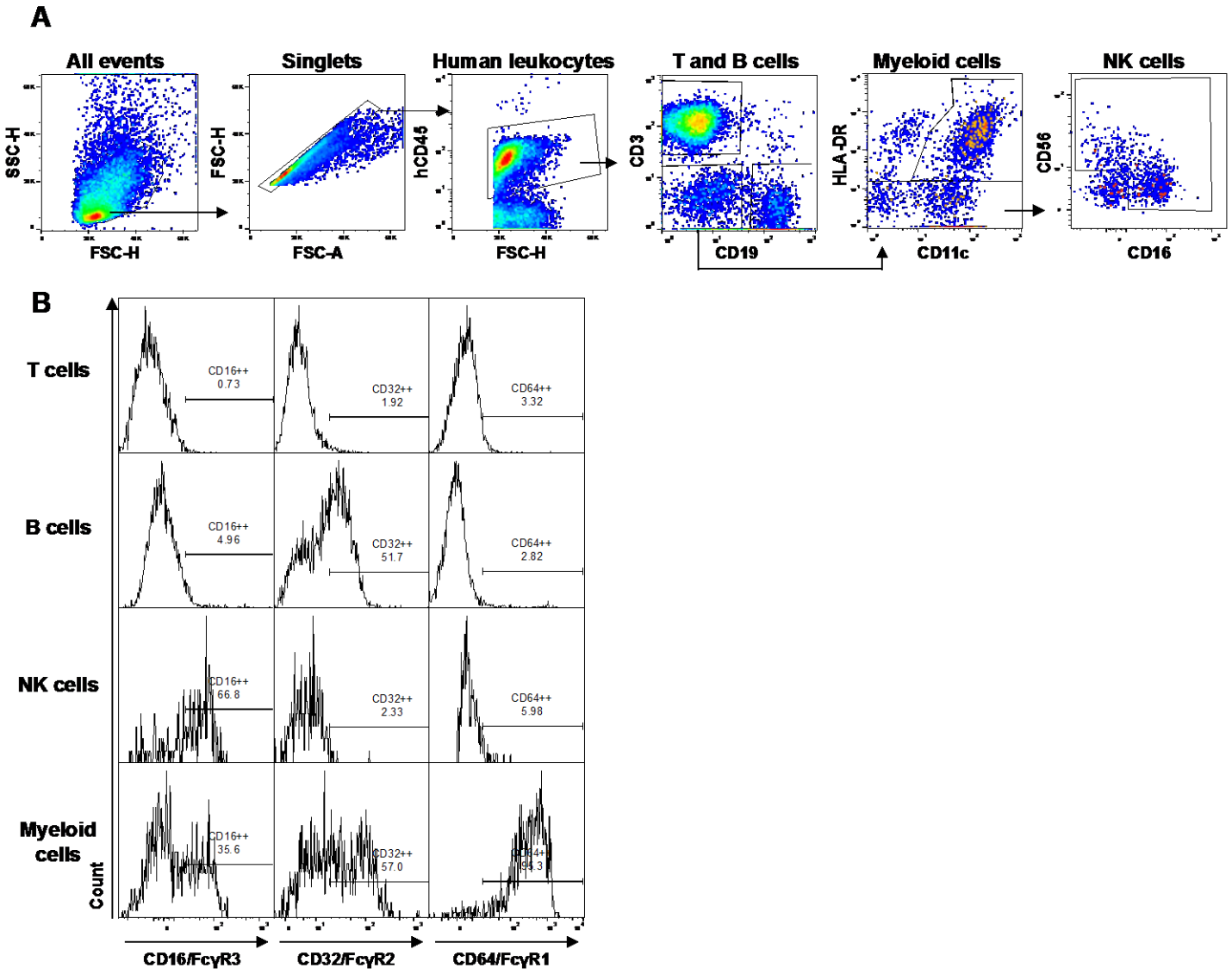

Figure S6. Gating strategy to determine FcγR expression on human immune cells in bone marrow-liver-thymus (BLT) mice.

(**A**) Gating strategy used to define human T and B cells, myeloid Cells, and NK Cells. A representative example is shown.

(**B**) The percentage of cells expressing each FcγR (CD16/32/64) protein within each subset shown in the representative example from (A).

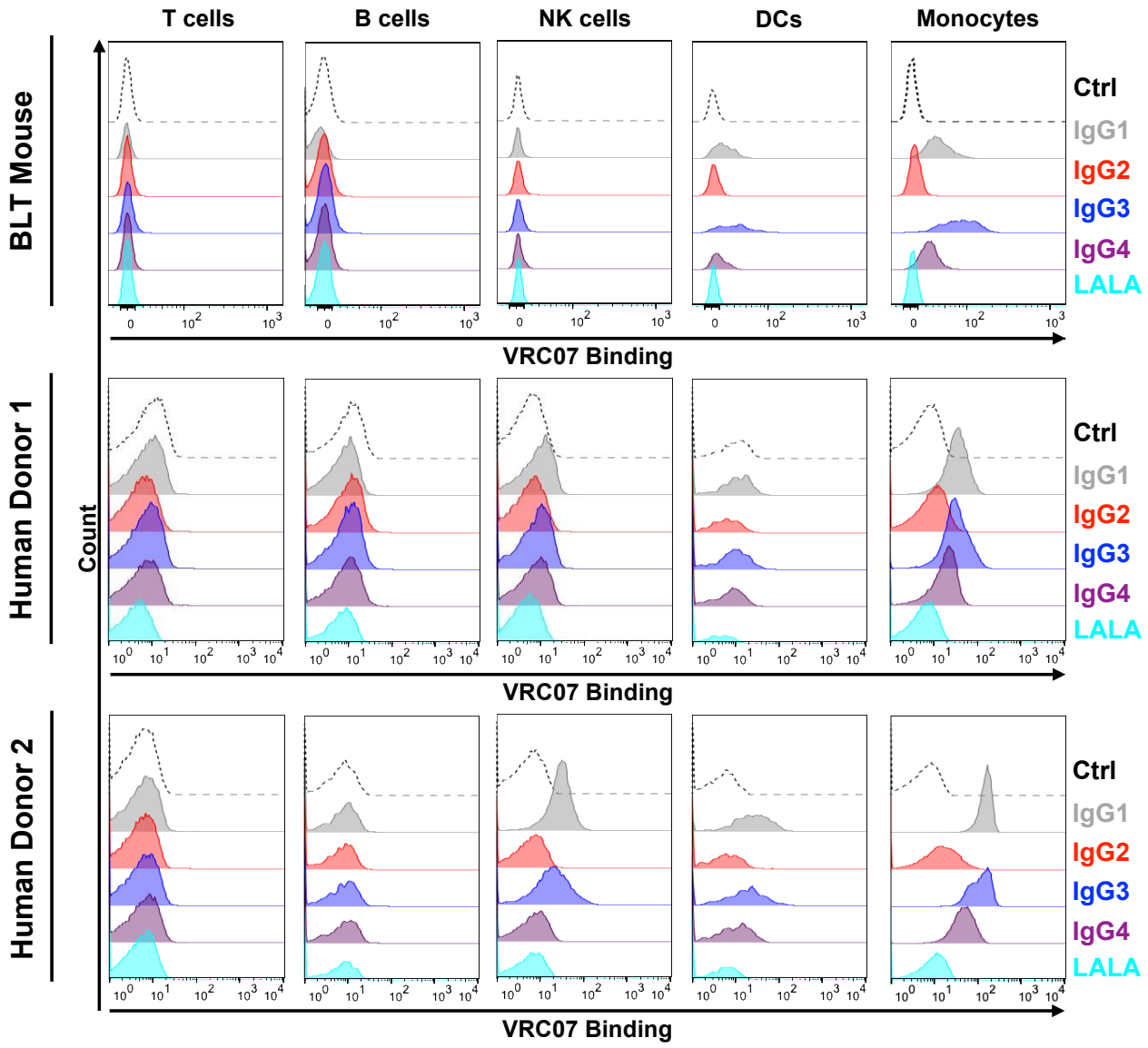

Figure S7. Binding of human immune cell subsets to VRC07 of each subclass.
Human immune cells were isolated from the spleen of a representative BLT humanized mouse or the peripheral blood of two different human donors and mixed with Alexa Fluor (AF) 647-labeled VRC07 Fc variants. Plots show VRC07 binding measured by flow cytometry for T cells ($CD45^+$, $CD3^+$), B cells ($CD45^+$, $CD20^+$), NK cells ($CD45^+$, $CD3^-$, $CD20^-$, $CD14^-$, $CD56^+$), dendritic cells (DCs; $CD45^+$, $CD3^-$, $CD20^-$, $CD56^-$, $CD16^-$, $HLA\text{-}DR^+$, $CD11c^+$), and monocytes ($CD45^+$, $CD3^-$, $CD56^-$, $CD14^+$).

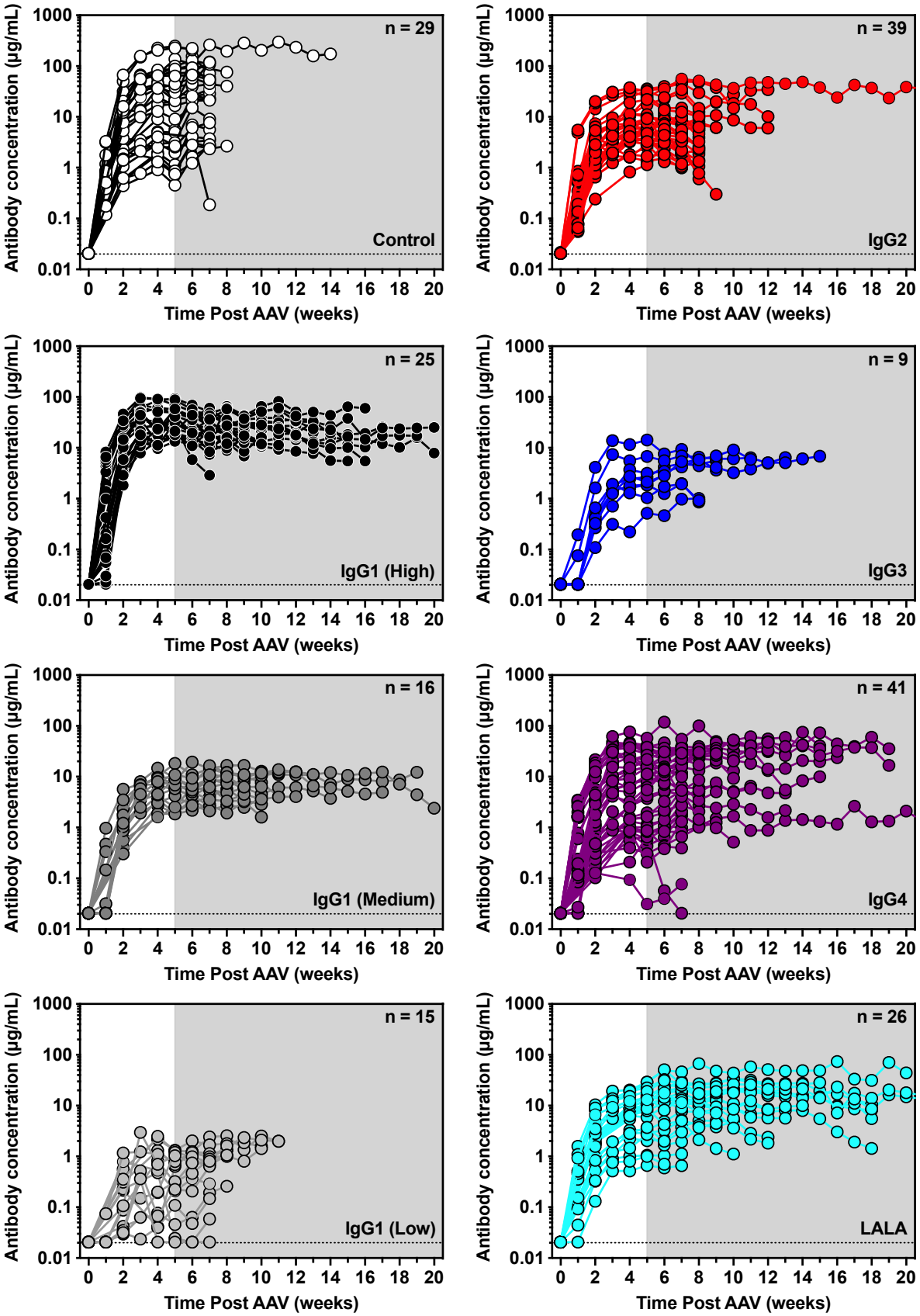

Figure S8. Antibody concentration of individual mice.
Antibody concentration (µg/mL) in the plasma of BLT humanized mice from the time of AAV injection until the time of HIV acquisition or death as measured by enzyme-linked immunosorbent assay (ELISA). The shaded region indicates the timing of weekly vaginal HIV challenges with 30 ng of p24 $HIV_{REJO.c}$, initiated at 5 weeks post-AAV administration. The dotted line indicates the limit of detection (0.0206 µg/mL) for the ELISAs.

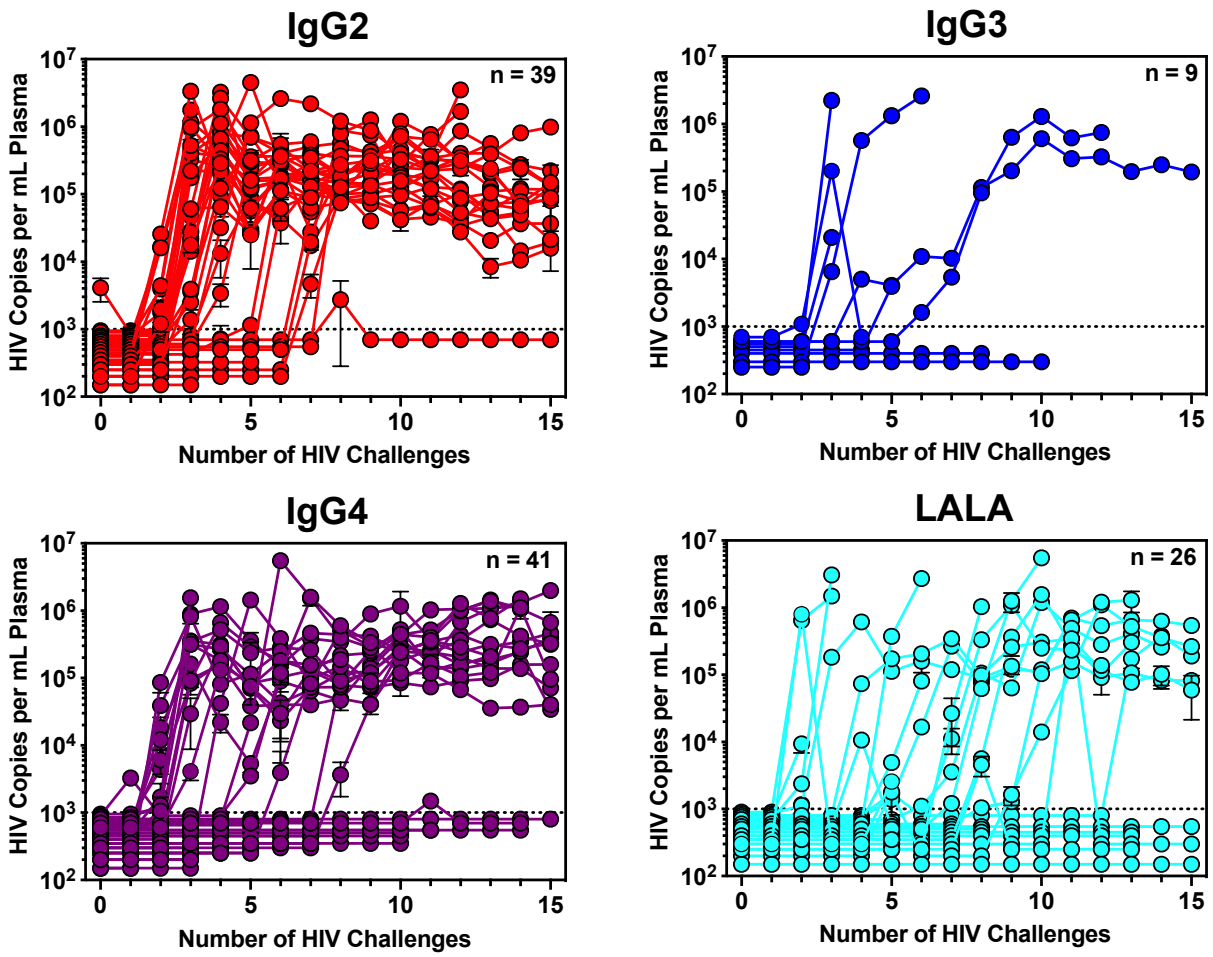

Figure S9. Viral Load of individual mice.
Viral load in the plasma of BLT humanized mice during repetitive challenge with 30 ng of p24 $HIV_{REJO.c}$ as measured by quantitative polymerase chain reaction (qPCR). The dotted line indicates the limit of detection (1000 copies/mL) for the assay. Samples with undetectable viral load were assigned an arbitrary value below the limit of detection. Error bars indicate standard deviation.

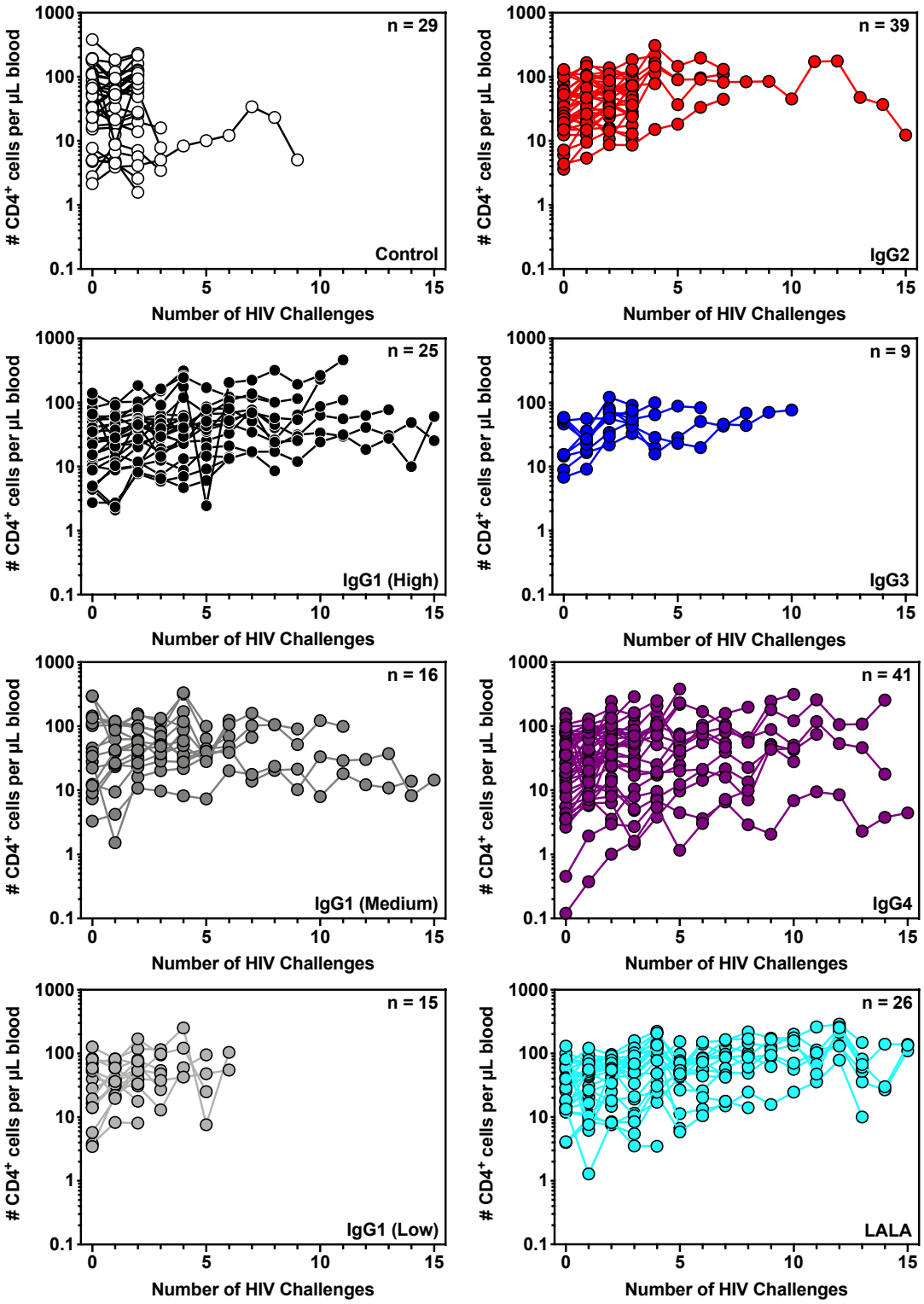

Figure S10. Number of human CD4⁺ cells in the peripheral blood of individual mice.
Number of human $CD3^+CD4^+$ cells in the peripheral blood of BLT humanized mice from the start of repetitive challenge with 30 ng of p24 $HIV_{REJO.c}$ until the time of HIV acquisition or death as measured by flow cytometry.

Table S1. Sequences of VRC07 antibodies.

VRC07 antibody sequences

VRC07 IgG1 heavy chain:

MATGSRTSLLLAFGLLCLPWLQEGSAQVRLSQSGGQMKKPGDSMRISCRASGYEFINCPINWIRLAPGKRPEWMGWMKPRGGAVSYARQLQGR
VTMTRDMYSETAFLELRSLTSDDTAVYFCTRGKYCTARDYYNWDFEHWGQGTPVTVSSASTKGPSVFPLAPSSKSTSGGTAALGCLVKDYFPE
PVTVSWNSGALTSGVHTFPAVLQSSGLYSLSSVVTVPSSSLGTQTYICNVNHKPSNTKVDKKVEPKSCDKTHTCPPCPAPELLGGPSVFLFPP
KPKDTLMISRTPEVTCVVVDVSHEDPEVKFNWYVDGVEVHNAKTKPREEQYNSTYRVVSVLTVLHQDWLNGKEYKCKVSNKALPAPIEKTISK
AKGQPREPQVYTLPPSRDELTKNQVSLTCLVKGFYPSDIAVEWESNGQPENNYKTTPPVLDSDGSFFLYSKLTVDKSRWQQGNVFSCSVMHEA
LHNHYTQKSLSLSPG

VRC07 IgG2 heavy chain:

MATGSRTSLLLAFGLLCLPWLQEGSAQVRLSQSGGQMKKPGDSMRISCRASGYEFINCPINWIRLAPGKRPEWMGWMKPRGGAVSYARQLQGR
VTMTRDMYSETAFLELRSLTSDDTAVYFCTRGKYCTARDYYNWDFEHWGQGTPVTVSSASTKGPSVFPLAPCSRSTSESTAALGCLVKDYFPE
PVTVSWNSGALTSGVHTFPAVLQSSGLYSLSSVVTVPSSNFGTQTYTCNVDHKPSNTKVDKTVERKCCVECPPCPAPPVAGPSVFLFPPKPKD
TLMISRTPEVTCVVVDVSHEDPEVQFNWYVDGVEVHNAKTKPREEQFNSTFRVVSVLTVVHQDWLNGKEYKCKVSNKGLPAPIEKTISKTKGQ
PREPQVYTLPPSREEMTKNQVSLTCLVKGFYPSDIAVEWESNGQPENNYNTTPPMLDSDGSFFLYSKLTVDKSRWQQGNVFSCSVMHEALHNH
YTQKSLSLSPG

VRC07 IgG3 heavy chain:

MATGSRTSLLLAFGLLCLPWLQEGSAQVRLSQSGGQMKKPGDSMRISCRASGYEFINCPINWIRLAPGKRPEWMGWMKPRGGAVSYARQLQGR
VTMTRDMYSETAFLELRSLTSDDTAVYFCTRGKYCTARDYYNWDFEHWGQGTPVTVSSASTKGPSVFPLAPCSRSTSGGTAALGCLVKDYFPE
PVTVSWNSGALTSGVHTFPAVLQSSGLYSLSSVVTVPSSSLGTQTYTCNVNHKPSNTKVDKRVELKTPLGDTTHTCPRCPEPKSCDTPPPCPR
CPEPKSCDTPPPCPRCPEPKSCDTPPPCPRCPAPELLGGPSVFLFPPKPKDTLMISRTPEVTCVVVDVSHEDPEVQFKWYVDGVEVHNAKTKP
REEQFNSTFRVVSVLTVLHQDWLNGKEYKCKVSNKALPAPIEKTISKTKGQPREPQVYTLPPSREEMTKNQVSLTCLVKGFYPSDIAVEWESS
GQPENNYNTTPPMLDSDGSFFLYSKLTVDKSRWQQGNIFSCSVMHEALHNRFTQKSLSLSPG

VRC07 IgG4 heavy chain:

MATGSRTSLLLAFGLLCLPWLQEGSAQVRLSQSGGQMKKPGDSMRISCRASGYEFINCPINWIRLAPGKRPEWMGWMKPRGGAVSYARQLQGR
VTMTRDMYSETAFLELRSLTSDDTAVYFCTRGKYCTARDYYNWDFEHWGQGTPVTVSSASTKGPSVFPLAPCSRSTSESTAALGCLVKDYFPE
PVTVSWNSGALTSGVHTFPAVLQSSGLYSLSSVVTVPSSSLGTKTYTCNVDHKPSNTKVDKRVESKYGPPCPSCPAPEFLGGPSVFLFPPKPK
DTLMISRTPEVTCVVVDVSQEDPEVQFNWYVDGVEVHNAKTKPREEQFNSTYRVVSVLTVLHQDWLNGKEYKCKVSNKGLPSSIEKTISKAKG
QPREPQVYTLPPSQEEMTKNQVSLTCLVKGFYPSDIAVEWESNGQPENNYKTTPPVLDSDGSFFLYSRLTVDKSRWQEGNVFSCSVMHEALHN
HYTQKSLSLSLG

VRC07 kappa light chain:

MATGSRTSLLLAFGLLCLPWLQEGSAEIVLTQSPGTLSLSPGETAIISCRTSQYGSLAWYQQRPGQAPRLVIYSGSTRAAGIPDRFSGSRWGP
DYNLTISNLESGDFGVYYCQQYEFFGQGTKVQVDIKRTVAAPSVFIFPPSDEQLKSGTASVVCLLNNFYPREAKVQWKVDNALQSGNSQESVT
EQDSKDSTYSLSSTLTLSKADYEKHKVYACEVTHQGLSSPVTKSFNRGEC

Table S2. Summary of animal numbers and treatment groups for three pooled BLT mouse experiments.

	Total Number	Number Per Treatment Group							
		Control	VRC07 IgG1 (High; >12µg/mL)	VRC07 IgG1 (Med; 2-12µg/mL)	VRC07 IgG1 (Low; <2µg/mL)	VRC07 IgG2	VRC07 IgG3	VRC07 IgG4	VRC07 LALA
Experiment 1	67	10	13	7	7	10	9	11	-
Experiment 2	65	9	11	3	-	15	-	15	12
Experiment 3	68	10	1	6	8	14	-	15	14

Data File S1 Legend

Figure 1 Tab:

Figure 1A. In vitro neutralization activity of purified VRC07 IgG subclasses against HIV_{JR-CSF} as measured by TZM-bl neutralization assays.

Figure 1B. Binding of VRC07 IgG subclasses or a malaria-specific negative control IgG1 antibody to HIV_{JR-CSF} Env-expressing target cells as measured by flow cytometry with a pan-IgG-Fc detection reagent.

Figure 1C. Half-maximal binding concentration (EC_{50}) of cell surface-bound VRC07 IgG subclasses to purified fluorescent-labeled FcγR proteins as measured by flow cytometry.

Figure 1D. Phagocytosis of HIV_{JR-CSF} Env-expressing target cells by THP-1 cells mediated by VRC07 IgG subclasses or a malaria-specific negative control IgG1 antibody as measured by flow cytometry.

Figure 1E and F. Ability of VRC07 IgG subclasses to mediate NK cell degranulation (top table) or specific killing of HIV_{JR-CSF} Env-expressing target cells (bottom table) as measured by flow cytometry.

Figure 2 Tab:

Figure 2B. In vitro neutralization activity of purified VRC07 IgG subclasses against HIV_{NL4-3} as measured by a TZM-bl neutralization assay.

Figure 2C. Plasma antibody concentrations (μg/mL) achieved in NSG mice following IM injection of 2.5×10^{11} genome copies (GC) of AAV expressing a given VRC07 IgG subclass or firefly luciferase as a negative control (Each column represents one mouse).

Figure 2D and E. CD4 depletion and viral load in the peripheral blood of huPBMC-NSG mice expressing firefly luciferase or a VRC07 IgG subclass following intravenous challenge of 280 $TCID_{50}$ HIV_{NL4-3}.

Figure 3 Tab:

Figure 3A. In vitro neutralization activity of purified VRC07 Fc variants or a malaria-specific negative control IgG1 antibody against $HIV_{REJO.c}$ as measured by TZM-bl neutralization assays.

Figure 3B. Binding of VRC07 IgG subclasses or a malaria-specific negative control IgG1 antibody to $HIV_{REJO.c}$ Env-expressing target cells as measured by flow cytometry with a pan-IgG-Fc detection reagent.

Figure 3C. Phagocytosis of $HIV_{REJO.c}$ Env-expressing target cells by THP-1 cells mediated by VRC07 Fc variants or a malaria-specific negative control IgG1 antibody as measured by flow cytometry.

Figure 3D and E. Ability of VRC07 Fc variants to mediate NK cell degranulation (top table) or specific killing of $HIV_{REJO.c}$ Env-expressing target cells (bottom table) as measured by flow cytometry.

Figure 4B to D Tab:

Figure 4B. The frequency of human T cells, B cells, NK cells, and myeloid cells in the peripheral blood of uninfected BLT mice 10 weeks post-surgical engraftment.

Figure 4C. Percentage of the human immune cell subsets expressing human FcγR1, FcγR2, or FcγR3 as measured by flow cytometry.

Figure 4D. Binding of AF647-labeled VRC07 Fc variants by human monocytes isolated from the spleens of BLT mice as measured by flow cytometry.

BLT Mouse Data (Figure 4 and 5) Tab:

Summary data for repetitive HIV vaginal challenge experiments in BLT humanized mice (Used in Figures 4 and 5).

Figure S3 Tab:

Figure S3. FcγR binding profiles for VRC07 IgG subclasses bound to $HIV_{JR\text{-}CSF}$ Env-expressing CEM.NKr cells as measured by flow cytometry.

Figure S4 Tab:

Figure S4A to C. Phagocytosis of $HIV_{JR\text{-}CSF}$, $HIV_{NL4\text{-}3}$, or $HIV_{REJO.c}$ gp120-coated fluorescent beads by THP-1 cells in the presence of different VRC07 IgG subclasses as measured by flow cytometry.

Figure S4D and E. Ability of VRC07 IgG subclasses to mediate NK cell degranulation (top table) and specific killing (bottom table) of $HIV_{JR\text{-}CSF}$ Env-expressing target cells as measured by flow cytometry.

Figure S5 Tab:

Figure S5A. In vitro neutralization activity of purified VRC07 IgG1 or LALA against $HIV_{JR\text{-}CSF}$ as measured by TZM-bl neutralization assays.

Figure S5B. Binding of VRC07 IgG1 or LALA to $HIV_{JR\text{-}CSF}$ Env-expressing target cells as measured by flow cytometry with a pan-IgG-Fc detection reagent.

Figure S8 Tab:

Figure S8. Antibody concentration (μg/mL) in the plasma of BLT humanized mice from the time of AAV injection until the time of HIV acquisition or death as measured by ELISA

Figure S9 Tab:

Figure S9. Viral load in the plasma of BLT humanized mice during repetitive challenge with 30 ng of p24 $HIV_{REJO.c}$ as measured by qPCR. Samples with undetectable viral load were assigned an arbitrary value below the limit of detection (1000 GC/mL).

Figure S10 Tab:

Figure S10. Number of human $CD3^{+}CD4^{+}$ cells in the peripheral blood of BLT humanized mice from the start of repetitive challenge with 30 ng of p24 $HIV_{REJO.c}$ until the time of HIV acquisition or death as measured by flow cytometry.